Supporting Information for

Two dimensional Janus Ti-trihalides monolayers with half-metallic characteristic, Mott insulator and tunable magnetic anisotropy

Xiaotian Fang[1], Baozeng Zhou[1], Xiaocha Wang[1,*], Wenbo Mi[2]

[1]Tianjin Key Laboratory of Film Electronic & Communicate Devices, School of Integrated Circuit Science and Engineering, Tianjin University of Technology, Tianjin 300384, China

[2]Tianjin Key Laboratory of Low Dimensional Materials Physics and Preparation Technology, School of Science, Tianjin University, Tianjin 300354, China


[*]Author to whom all correspondence should be addressed.

E-mail: wangxc@email.tjut.edu.cn

Table S1. The bond lengths (d_1, d_2) and bond angles (θ_1, θ_2) of each monolayer. Local magnetic moments of Ti/Cr ($M_{\text{Ti}}/M_{\text{Cr}}$) and X/Y (M_X/M_Y) atoms.

	d_1 (Å)	d_2 (Å)	θ_1 (°)	θ_2 (°)	M_{Ti} (μ_B)	M_X (μ_B)	M_Y (μ_B)
TiI$_3$	2.833	2.833	92.224	92.224	1.067	-0.031	-0.031
Ti$_2$Br$_3$I$_3$	2.627	2.824	98.251	89.375	1.054	-0.023	-0.032
Ti$_2$Cl$_3$I$_3$	2.481	2.821	104.063	87.779	1.046	-0.018	-0.033
Ti$_2$Cl$_3$Br$_3$	2.464	2.609	98.224	91.107	1.023	-0.018	-0.022
TiCl$_3$	2.457	2.457	94.855	94.855	1.011	-0.017	-0.017
	d_1 (Å)	d_2 (Å)	θ_1 (°)	θ_2 (°)	M_{Cr} (μ_B)	M_X (μ_B)	M_Y (μ_B)
CrI$_3$	2.747	2.747	92.772	92.772	3.400	-0.134	-0.134
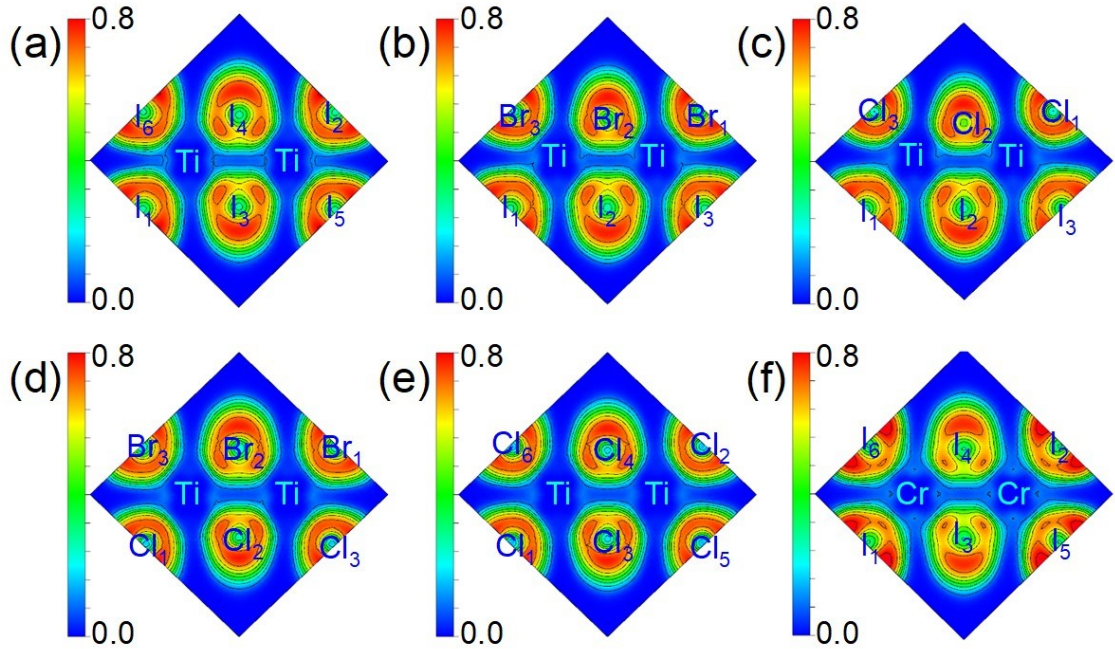
Fig. S1. ELF of the (a) TiI3, (b) Ti$_2$Br$_3$I$_3$, (c) Ti$_2$Cl$_3$I$_3$, (d) Ti$_2$Cl$_3$Br$_3$, (e) TiCl$_3$, (f) CrI$_3$ monolayer. ELF=1 (read) and 0 (blue) indicate the accumulation and depletion of electron density, respectively, and the range chosen here is 0 to 0.8.
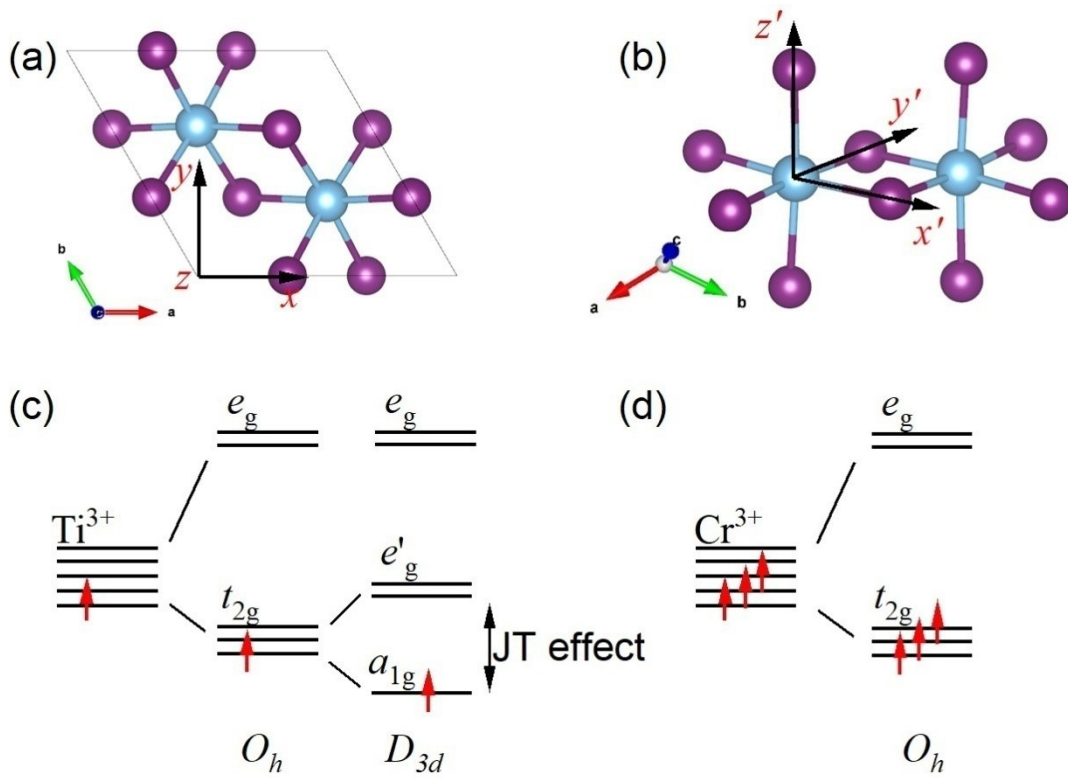
Fig. S2. Edge-sharing TiI_6 octahedra with (a) the global xyz coordinate system and (b) the local $x'y'z'$ coordinate system. The crystal field splitting of d levels in (c) Ti $3d^1$ and (d) Cr $3d^3$.
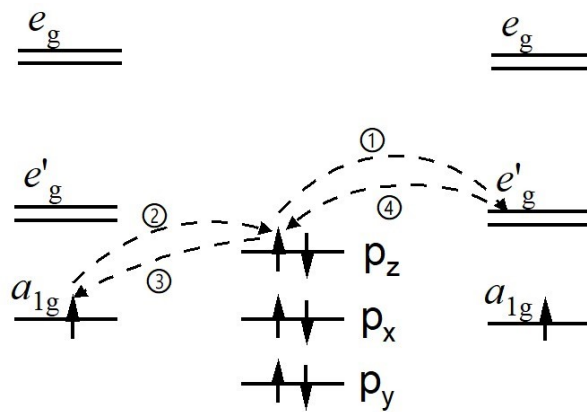
Fig. S3. Schematic plot of FM superexchange interactions in TiI_3 monolayer.
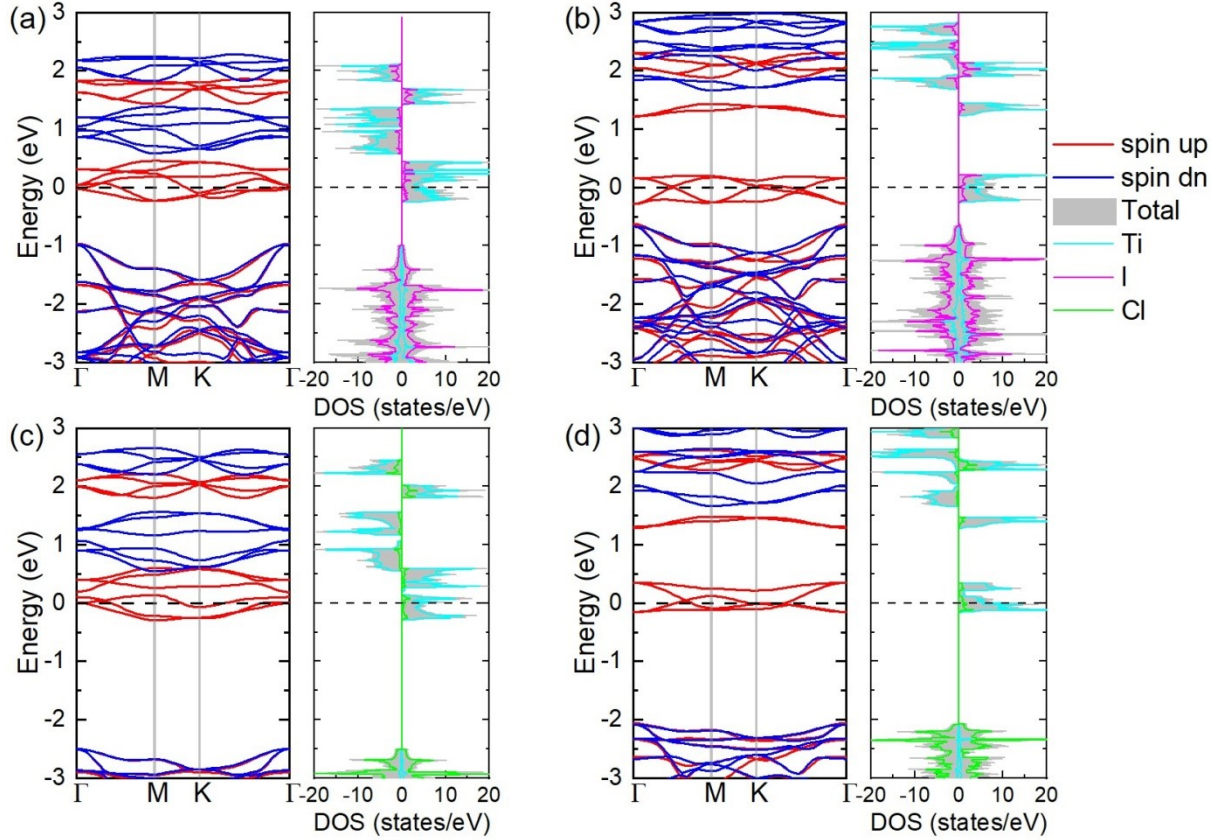
Fig. S4. The band structure and PDOS of the half-metallic state with (a) t_{2g}^{1} and (b) $e'_{g}{}^{1}a_{1g}{}^{0}$ configurations for TiI_3 monolayer. The band structure and PDOS of the half-metallic state with (c) t_{2g}^{1} and (d) $e'_{g}{}^{1}a_{1g}{}^{0}$ configurations for $TiCl_3$ monolayer.

Two different half-metallic states were obtained by the PBE and the occupation-matrix-control PBE+U_{eff} method in Fig. S4. The steps of the occupation-matrix-control PBE+U_{eff} method are described. First of all, occupation-matrix-control PBE+U_{eff} starts structure optimization with input file OCCMATRIX initializing the occupancy density matrix. Then, the relaxed structure is used to perform a self-consistent-field (SCF) calculation with occupation control. The output CHGCAR and WAVECAR are read for a next relaxation without occupation control. Finally, the relaxed structure is used for the SCF calculation (this usually also requires a step of occupation control calculation first, e.g. reading the occupation density matrix output from the previous step, otherwise the expected electronic structure may not be obtained).

It should be pointed out that the complete SCF PBE+U_{eff} calculation without occupation control can also obtain twin orbital-order phases, but this is relatively difficult because the self-consistent solution often depends on the parameter settings.[1-3] Following is the CONTCAR file (used for VASP) for $a_{1g}^1 e'^0_g$ and $e'^1_g a_{1g}^0$ configurations of the TiCl$_3$ monolayer in a complete SCF PBE+U_{eff} calculation.

$a_{1g}^1 e'^0_g$ electronic configuration

1.00000000000000

   6.2681495088052177   0.0000000000000000   0.0000000000000000

  -3.1340747544026133   5.4283767093442652   0.0000000000000000

   0.0000000000000000   0.0000000000000000 20.0000000000000000

  Cl   Ti

   6   2

Direct

0.0000000000000000 0.6435794387893308 0.4301205835494915

0.0000000000000000 0.3564205612106697 0.5698794164505085

0.3564205612106697 0.3564205612106697 0.4301205835494915

0.6435794387893308 0.6435794387893308 0.5698794164505085

0.6435794387893308 0.0000000000000000 0.4301205835494915

0.3564205612106697 0.0000000000000000 0.5698794164505085

0.3333333333333333 0.6666666666666666 0.5000000000000000

0.6666666666666667 0.3333333333333334 0.5000000000000000

$e'^1_g a_{1g}^0$ electronic configuration

1.00000000000000

6.1086044213302273   0.0000000000000000   0.0000000000000000

-3.0543022106651172   5.2902066105419117   0.0000000000000000

0.0000000000000000   0.0000000000000000   20.0000000000000000

Cl   Ti

6   2

Direct

0.0000000000000000   0.6589168856719224   0.4299829405071204

0.0000000000000000   0.3410831143280780   0.5700170594928793

0.3410831143280780   0.3410831143280780   0.4299829405071204

0.6589168856719224   0.6589168856719224   0.5700170594928793

0.6589168856719224   0.0000000000000000   0.4299829405071204

0.3410831143280780   0.0000000000000000   0.5700170594928793

0.3333333333333333   0.6666666666666666   0.5000000000000000

0.6666666666666667   0.3333333333333334   0.5000000000000000

One can perform SCF calculations with these two relaxed structures, and the results are consistent with those of the occupation-matrix-control PBE+U_{eff} method.
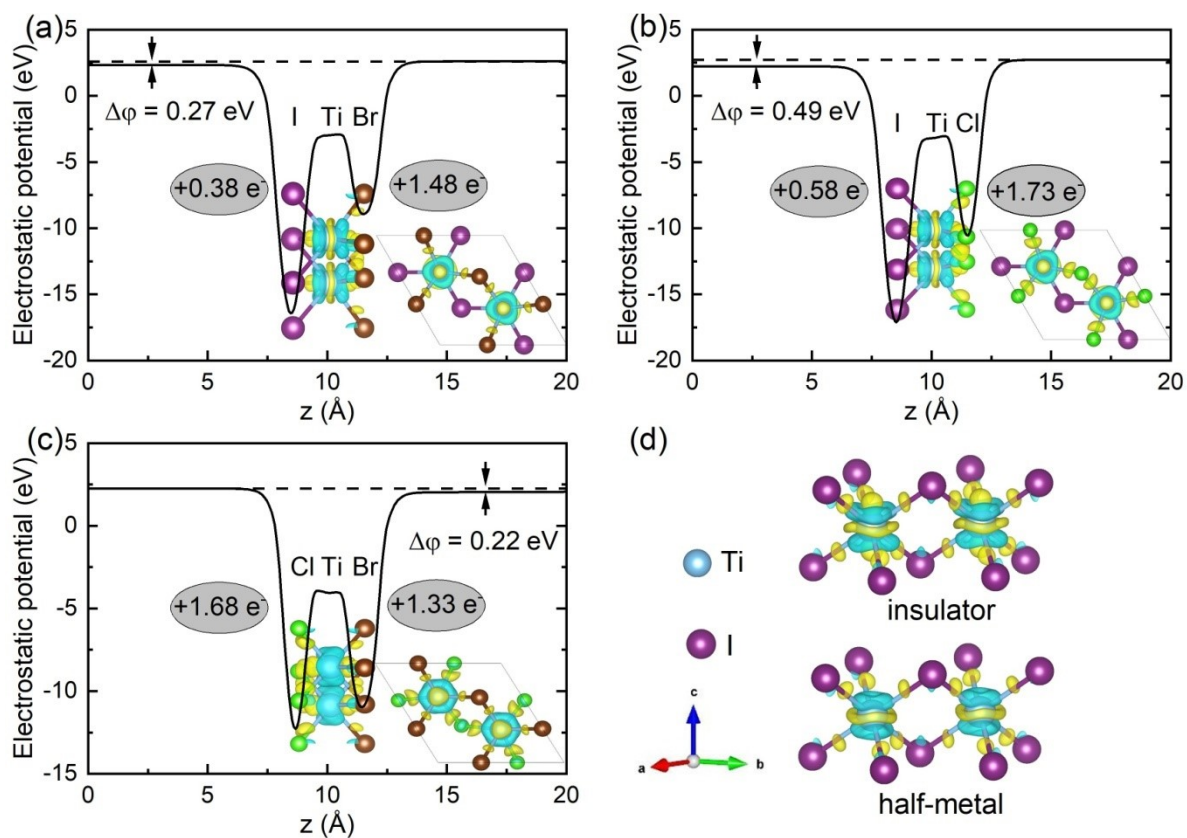
Fig. S5. Electrostatic potential energy and differential charge density of the Janus (a) $Ti_2Br_3I_3$, (b) $Ti_2Cl_3I_3$ and (c) $Ti_2Cl_3Br_3$ monolayers. $\Delta\varphi$ is the electrostatic potential difference and the value of isosurface is set to 0.015 $e/Bohr^3$. (d) Differential charge density of the TiI_3 monolayer, where the value of isosurface is set to 0.01 $e/Bohr^3$. Yellow and blue regions represent charge gain and loss, respectively.
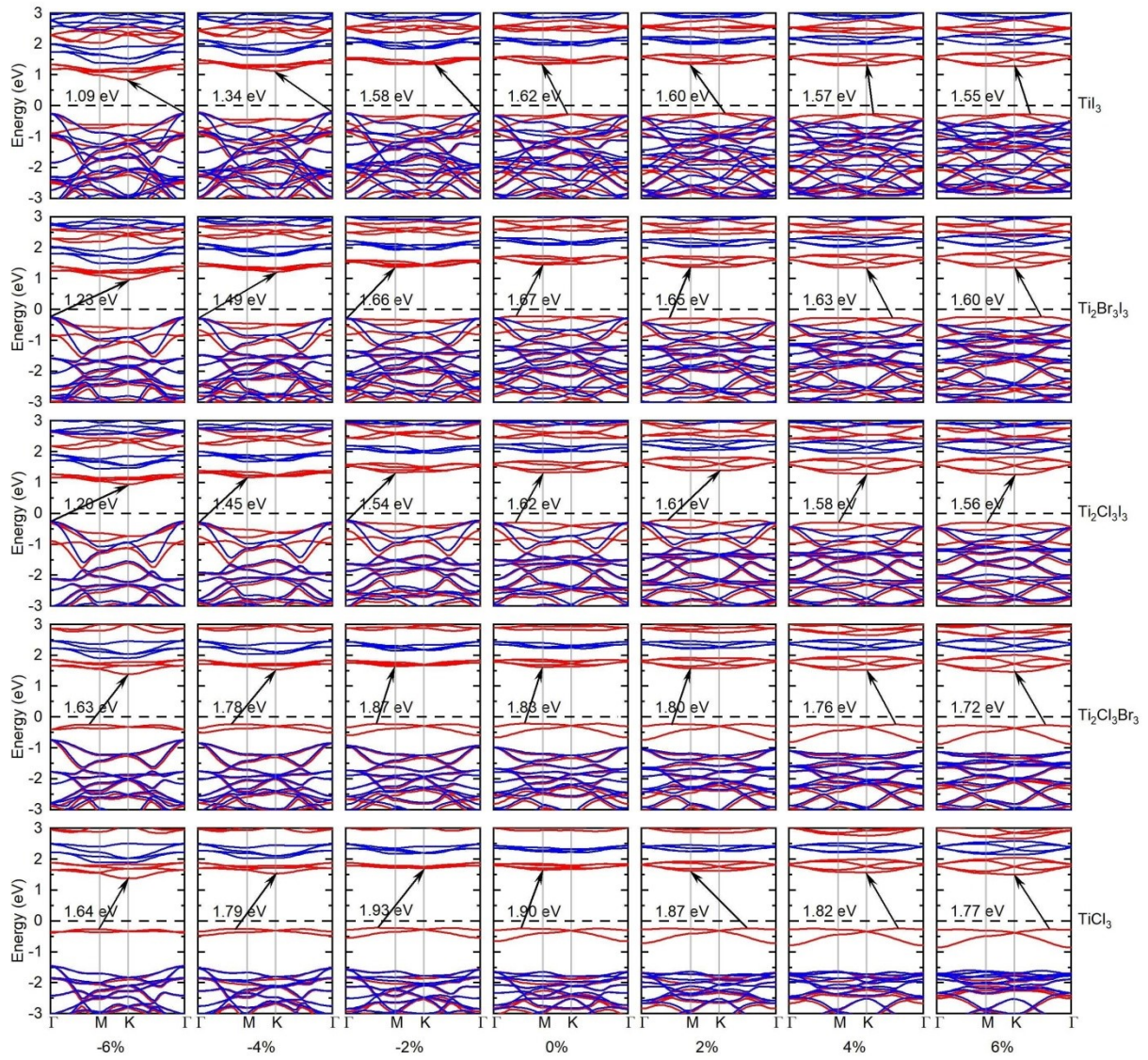
Fig. S6. The band structures of $Ti_2X_3Y_3$ monolayers at in-plane biaxial strain of -6% to 6%.

References

1. B. Meredig, A. Thompson, H. A. Hansen, C. Wolverton and A. van de Walle, *Phys. Rev. B*, 2010, **82**, 195128.

2. X. Fang, B. Zhou, N. Sun, L. Fu and X. Wang, *Phys. Chem. Chem. Phys.*, 2022, **24**, 4374-4383.

3. Y. P. Wang and M. Q. Long, *Phys. Rev. B*, 2020, **101**, 024411.